Relating the Microscopic and Macroscopic Response of a Polymeric Fluid in a Shearing Flow

Hazen P. Babcock,[1] Douglas E. Smith,[1] Joe S. Hur,[2] Eric S. G. Shaqfeh,[2] and Steven Chu[1]
[1]*Departments of Physics and Applied Physics, Stanford University, Stanford, California 94305*
[2]*Department of Chemical Engineering, Stanford University, Stanford, California 94305*
(Received 9 March 2000)

The microscopic and macroscopic response of a polymer solution in start-up shear flow was investigated using fluorescence microscopy of single molecules, bulk viscosity measurements, and Brownian dynamics simulations. An overshoot in viscosity was observed upon flow inception and understood via the observed molecular extension and by simulation findings. Increasing the polymer concentration up to six times the overlap concentration (C^*) has no effect on the character of the dynamics of individual molecules.

PACS numbers: 83.10.Nn, 87.14.Gg, 87.15.–v

One of the most important goals in understanding complex fluids is to link the macroscopic material properties with microscopic changes. For instance, interesting macroscopic responses of these complex fluids containing large molecules such as polymers, colloids, liquid crystals, micelles, and surfactants have been widely reported in the literature [1–7]. A classic example is the observation that polymeric fluids often display a transient overshoot in viscosity upon the inception of a shearing flow [5–7]. Various theories and models predict such an overshoot [8–13] but a clear understanding of how this macroscopic behavior is associated with the changes in microscopic state is lacking.

In this work, we made detailed observations of both the molecular dynamics and the macroscopic viscosity of the same polymer solution. The effect of concentration was studied down to nearly infinite dilution in order to distinguish individual chain effects from those due to intermolecular interactions [14]. Finally, the experimental data were compared to the predictions of molecular models specifically based on the known molecular parameters of the polymer used in the experiments. We used DNA solutions as a model system and made side-by-side comparison of the single-molecule observations, viscosity measurements, and Brownian dynamics simulations.

Simple shear flow was created in a ~ 50 μm gap between two parallel glass plates in an apparatus similar to that used previously [15,16]. We measured the maximum extension of the polymers in the flow direction (direction of plate travel) using video fluorescence microscopy. The technique has been improved such that the transient molecular extension could be observed in the center-of-mass frame of a single molecule during the start-up of shear flow. In order to visualize single molecule dynamics at higher polymer concentrations, small fractions of fluorescently labeled "probe" molecules were added to solutions of unlabeled molecules [17–20]. To determine the statistical properties of the molecular dynamics, these measurements were repeated on an "ensemble" of 60 to 130 identical molecules for each different shear rate and sample concentration. The time-dependent shear viscosity of the same DNA solutions was measured using a rheometer (RDA II, RSI Scientific, Piscataway, NJ).

By observing the recoil of isolated, stretched molecules after the flow is turned off we measure the longest relaxation time, τ, of our polymer [21]. The dimensionless parameter called the "Weissenberg Number" Wi is used to characterize the effective strength of the shear flow. It is the product $\dot{\gamma}\tau$ where $\dot{\gamma}$, the shear rate, is the plate velocity divided by the gap width. In the simplest case of an isolated chain, one generally expects the statistical properties of two data sets, even if they are taken at different solvent viscosities, to match as long as Wi is the same for both [15,22]. At higher concentrations one eventually expects to see deviations due to strong intermolecular interactions (in particular, entanglements) which should change the character of the dynamics.

First, we considered the limit of infinite dilution in order to examine the polymer response in the absence of any possible interactions between polymer molecules. We used a concentration of $10^{-5}C^*$ [23]. At this concentration the average distance between molecules is much larger than the contour length of a molecule and we expect interactions to be negligible. When there is no applied flow, flexible polymers adopt a random coil state. If a shear flow is suddenly applied the polymers begin to stretch. While the individual polymers display widely different dynamics upon flow inception, the average extension rises smoothly to a constant steady state value [Fig. (1)]. For Wi > 19, we observed a small overshoot in extension.

In order to test whether the overshoot in extension was due to an initial time synchronization of coiled molecules, we compared the dynamics of coiled molecules stretching at the inception of flow to the dynamics of transiently coiled chains after steady-state conditions had been reached. We set the new time $= 0$ point to be the first point in the time trace after 50 strain units where the polymer extension was less than one standard deviation from the average extension at Wi $= 0$. When these traces were averaged together, there was no evidence of an overshoot.

 0031-9007/00/85(9)/2018(4)$15.00

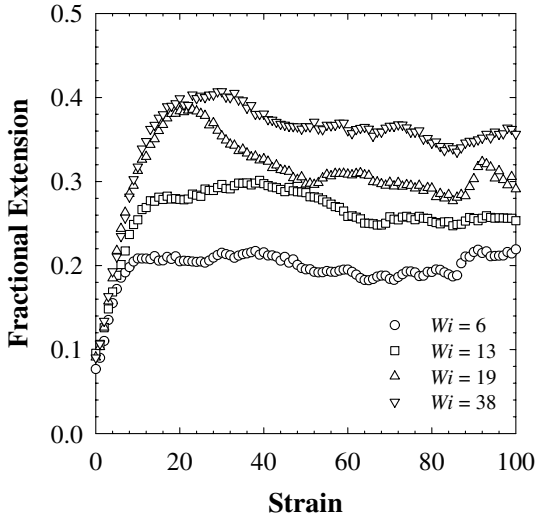

FIG. 1. The ensemble average response was calculated by averaging all the individual traces taken at the same Wi number together. The fractional extension is defined as the ratio of maximum chain extension to the contour length of the molecule.

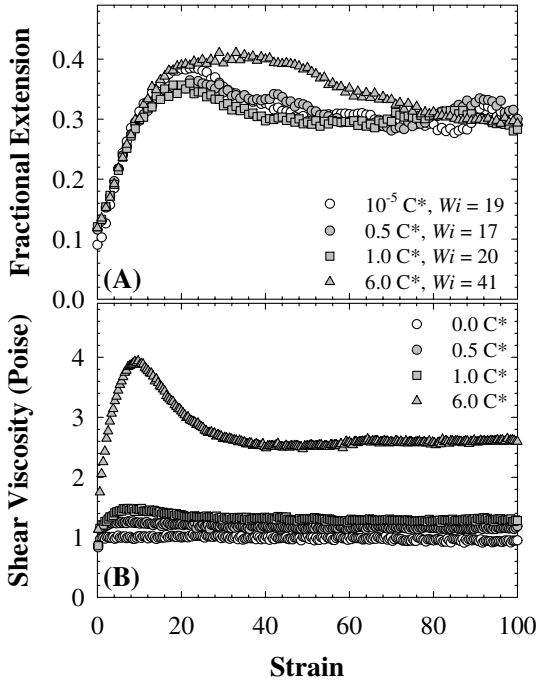

FIG. 2. (A) A plot of the average fractional extension versus strain at different DNA concentrations. (B) Measurements of the shear viscosity of solutions of the same composition used in the single molecule measurements. These measurements were all made at a shear rate of 1.32 s^{-1}. Traces are the average over eight data sets taken from four separately prepared samples.

This finding strongly suggests that the overshoot arises from the initial alignment of the coiled conformation with the flow and not just an initial temporal synchronization of stretching chains.

To test the effect of intermolecular interactions, measurements were done at concentrations of $0.5C^*$, $1.0C^*$, and $6.0C^*$ [Fig. (2)]. These concentrations lie in or near the so-called "semidilute" regime. The highest concentration examined in this study, $6.0C^*$, is a factor of ~ 2 smaller than the concentration at which full reptation is observed [24,25]. At a concentration of $6.0C^*$ polymer-polymer interactions increased the measured relaxation time of a single polymer to 2.5 times that of an isolated polymer at a concentration of $10^{-5}C^*$. Surprisingly, the time at which the overshoot in extension occurs and its magnitude are the same as that for a dilute solution of the same Wi. The fact that the average extensions at different concentrations are similar in character when compared at the same Wi suggests that the effect of these semidilute interactions may be modeled (in a mean field sense) as an effective viscous medium.

The macroscopic shear viscosity of the same solutions used for the single-molecule measurements was measured with a shear viscometer. Figure (2)B, shows the shear viscosity as a function of strain for 4 different polymer concentrations. As the polymer concentration is increased, the size of the overshoot in total shear viscosity increases, going from 1 for pure solvent to 4× the solvent viscosity at $6.0C^*$. We find that the overshoot in shear viscosity precedes the overshoot in polymer extension at all shear rates and concentrations. Our single molecule data [Fig. (2)] suggest that the viscosity overshoot is not due to polymer-polymer interactions. The marked increase in the size of the overshoot in shear viscosity with polymer concentration is consistent with polymer-solvent interactions being dominant, since the amplitude of the viscosity overshoot relative to the solvent viscosity increases linearly with polymer concentration [Fig. (3)].

To better understand the relationship between the overshoot in viscosity and extension, we used Brownian dynamics simulations of Kramers' bead-rod chains [Fig. (4)] [26–29]. From the calculated chain configurations in the model, one can calculate the resulting polymer shear viscosity using the standard Kramers stress formula [30].

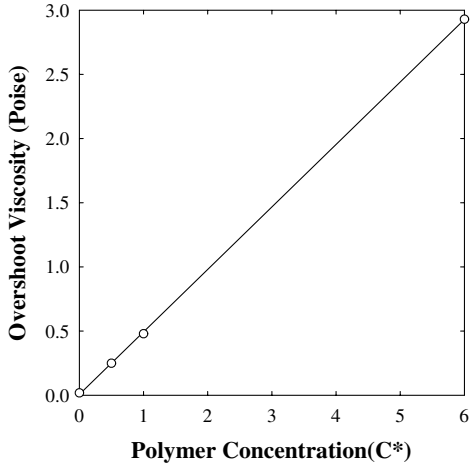

FIG. 3. A plot of the maximum viscosity (the viscosity at the overshoot) after subtracting the solvent viscosity versus polymer concentration.

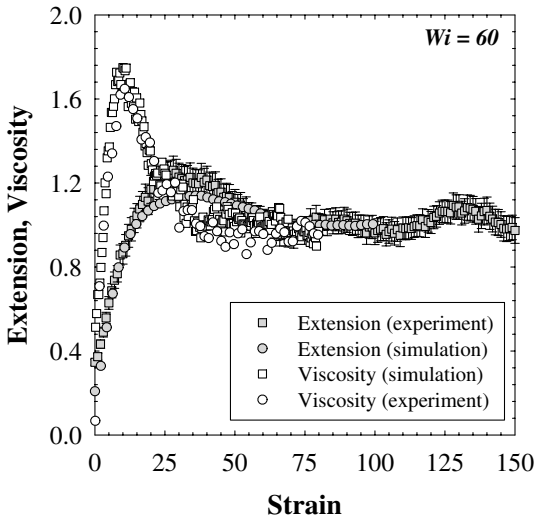

FIG. 4. The polymer shear viscosity and the molecular extension of 150 bead Kramers chains for Wi = 60 were calculated from an ensemble of 400 independent chains. All chains started from independent equilibrium states before the inception of shear flow in the simulation. We normalized the polymer shear viscosity with the steady polymer shear viscosity and the molecular extension with the steady chain length at Wi = 60. For comparison normalized experimental values of the polymer shear viscosity and molecular extension of the $1C^*$ DNA solution are plotted. The apparent quantitive difference in molecular extension between simulation and experiment is smaller than the noise in the experiment, which can be estimated by the size of the fluctuations at steady-state (strain >100).

For example, in shear flow chainlike molecules aligned perpendicular to the flow direction (that is, the "gradient" direction) contribute greater hydrodynamic friction than chains aligned parallel to the flow direction. The steady-state shear viscosity is thus directly related to the average chain thickness in the gradient direction.

It is found that the overshoot in both molecular extension and shear viscosity is due to nonaffine deformation at Wi $>$ 20 [31]. In the simulation, we observe that the chain is initially stretched along the principal axis (45° relative to the flow direction) of stretching before it starts to align with the flow. The chain starts to unravel in the flow direction and initially the chain thickness in the gradient direction remains the same. As the chain gets more highly extended it starts to rotate to the stagnation line (parallel to the motion of the plates) at high flow strength (Wi $>$ 20). This leads to a reduction in the chain thickness in the gradient direction and thus less resistance is felt by the nearby solvent molecules. During this transition time, the shear viscosity initially grows due to chain expansion (from a coiled to an extended state) and starts to decrease as the chain starts to rotate and align with the flow. As the chain becomes aligned, there is no relative velocity between the chain segments, and the chain retracts. The maximum overshoot in shear viscosity occurs at the point where the chain begins to rotate to the stagnation line (when the chain extends over the largest velocity gradient). The peak overshoot in molecular extension occurs when the chain has come down to near the stagnation line. We note that the chain thickness in the gradient direction does not decrease for Wi $<$ 10, thus no overshoot in both shear viscosity or extension is observed.

The dependence of the steady-state properties on concentration was also investigated. We found that at DNA concentrations of $6.0C^*$ and smaller there is no measurable difference between the mean extension at $10^{-5}C^*$ and those at higher polymer concentrations. Histograms of the fractional extension showed little change as a function of concentration at the same Wi number. In contrast, light scattering measurements on polystyrene solutions (at Wi $<$ 2.5), showed an approximately 40% increase in radius of gyration as the concentration was increased from $0.05C^*$ to $0.75C^*$ [32,33].

We also calculated the power spectra characterizing the extensional fluctuations in steady shear flow [15,34]. One eventually expects the power spectra to change as the concentration increases because of the effect of the intermolecular entanglements [35]. The power spectral density (PSD) calculated for $10^{-5}C^*$, $0.5C^*$, and $1.0C^*$ and a shear rate of 1.32 s^{-1} corresponding to a narrow range of comparable Wi (= 16–20) collapse on top of each other [Fig. (5)]. The experimental PSD also agree with those calculated from a 150 bead Kramers' chain in our Brownian dynamics simulations where the number of Kuhn steps matched that of the λ-DNA molecules [29]. All the data show a plateau at the lowest frequencies followed by a sharp decay at intermediate frequencies, and finally a less pronounced decay at higher frequencies. The power spectra for $6.0C^*$ solutions do not

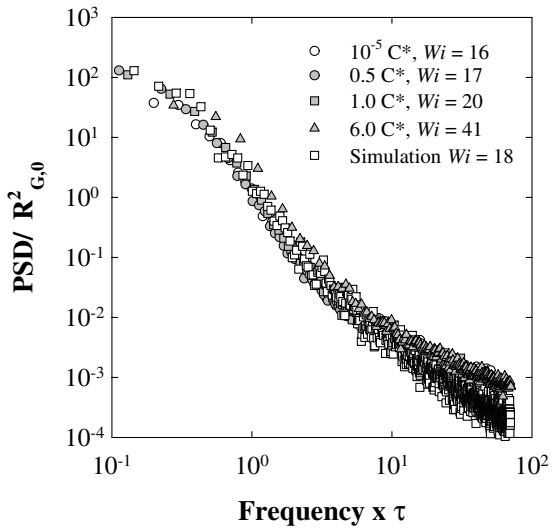

FIG. 5. The power spectral density (PSD) of the extension fluctuations at steady state for various values of background polymer concentration. All the PSDs were made dimensionless with the known equilibrium radius of gyration R_g and the longest polymer relaxation time τ. In the simulation the extension of one chain as a function of time was collected after it equilibrated in steady shear flow and its dimensionless PSD was calculated following the same procedure as that used for the experiment.

overlap with those taken at lower concentrations and at the same shear rate. However the $6.0C^*$ power spectrum does overlap with the PSD characterizing the dynamics in dilute solution at the same value of Wi (data not shown).

We have demonstrated how one can establish a direct connection between macroscopic properties and measured microscopic behavior by studying the dynamics of polymers in start-up and steady shear flow. In future work it is expected that multichain dynamic simulations may be used to investigate the origins of the weak concentration dependence on single chain behavior. It is also of great interest to investigate single molecule dynamics in solution at much greater concentrations to examine the crossover to reptative behavior ($>10C^*$). A study of the concentration effects on the dynamics in other types of flow may also provide insight into the effects of polymer-polymer interactions.

This work was supported in part by the U.S. AFOSR and the NSF. D. E. S. received support from the NSF Program in Mathematics and Molecular Biology. H. P. B. was supported in part by an NIH biophysics training grant and in part by CPIMA. J. S. H. and E. S. G. S. were funded by NSF under CPIMA Cooperative Agreement No. DMR-9808677.

[1] X. J. Fan, J. Non-Newt. Fluid Mech. **17**, 125 (1985).
[2] J. F. Berret, Langmuir **13**, 2227 (1997).
[3] K. Nakai *et al.,* J. Chem. Soc. Faraday. Trans. **89**, 2467 (1993).
[4] T. C. B. Mcleish *et al.,* Macromolecules **32**, 6734 (1999).
[5] T. Kume, T. Hattori, and T. Hashimoto, Macromolecules **30**, 427 (1997).
[6] J. J. Magda *et al.,* Macromolecules **26**, 1696 (1993).
[7] A. W. Chow *et al.,* Macromolecules **18**, 805 (1985).
[8] B. H. A. A. vandenBrule, J. Non-Newt. Fluid Mech. **47**, 357 (1993).
[9] A. P. G. vanHeel, M. A. Hulsen, and B. H. A. A. vandenBrule, J. Non-Newt. Fluid Mech. **75**, 253 (1998).
[10] M. Herrechen and H. C. Öttinger, J. Non-Newt. Fluid Mech. **68**, 17 (1997).
[11] P. S. Doyle and E. S. G. Shaqfeh, J. Non-Newt. Fluid Mech. **76**, 43 (1998).
[12] C. C. Hua, J. D. Schieber, and D. C. Venerus, J. Rheol. **43**, 701 (1999).
[13] W. Carl, Rheol. Acta **36**, 197 (1997).
[14] R. C.-Y. Ng and L. G. Leal, J. Rheol. **37**, 443 (1993).
[15] D. E. Smith, H. P. Babcock, and S. Chu, Science **283**, 1724 (1999).
[16] A new apparatus was built for this experiment that used a smaller volume of fluid, approximately 1 ml. The top plate was a 1.9 cm $\times$ 0.3 cm $\times$ 0.1 cm piece of glass and the channel had dimensions of 3.7 cm $\times$ 0.9 cm.
[17] YOYO-1 (Molecular Probes, Eugene OR) was mixed with λ-DNA (Gibco BRL, Gaithersburg, MD) at a dye/base pair ratio of 1:4. The contour length of λ-DNA stained with this dye concentration is 22 μm.
[18] All of the Wi = 6, 13, 19, and 39 data sets were taken in the sucrose/glucose buffer made as described previously [15].
[19] Solutions were made with 65%(w/w) sucrose, 10%(w/w) glucose, 10 mM tris-HCl pH 8.5, 1 mM EDTA, 10 mM NaCl, and the appropriate amount of λ-DNA stock solution to achieve the desired concentration of unlabeled molecules. When the buffer fraction of λ-DNA was replaced with water, these solutions had a viscosity of 100cP.
[20] An oxygen scavenging system with the following final concentrations was used to reduce photobleaching. 1% β-mercaptoethanol, 0.05 mg/ml glucose oxidase, and 0.01 mg/ml catalase.
[21] τ was determined by fitting to the function $x(t)^2 = c\exp^{(-\frac{t}{\tau})} + 6\,\mathrm{Rg}^2$ and was averaged over >40 molecules. For the 60 cP (τ = 6.3 s) and 200 cP (τ = 19 s) buffers relaxation times were the same as those measured in [15]. In the 100 cP $10^{-5}C^*$, $0.5C^*$, $1.0C^*$, and $6.0C^*$ the relaxation times were 12, 13, 15, and 31 s, respectively.
[22] This assumes that the solvent quality is similar at different solvent viscosities, which is true for the sugar solutions used for these experiments [15].
[23] For λ-DNA 1.0 C^* corresponds to a concentration of 0.04 mg/ml based on a measured radius of gyration of 0.7 μm. We note that C^* as calculated from intrinsic viscosity measurements is reported to be approximately 6$\times$ less than C^* calculated by radius of gyration [R. G. Larson, *The Structure and Rheology of Complex Fluids* (Oxford University Press, Oxford, 1999)].
[24] D. E. Smith, T. T. Perkins, and S. Chu, Phys. Rev. Lett. **75**, 4146 (1995).
[25] T. T. Perkins, D. E. Smith, and S. Chu, Science **264**, 819 (1994).
[26] T. W. Liu, J. Chem. Phys. **90**, 5826 (1989).
[27] P. S. Doyle, E. S. G. Shaqfeh, and A. P. Gast, J. Fluid Mech. **334**, 251 (1997).
[28] D. Petera and M. Muthukumar, J. Chem. Phys. **111**, 7614 (1999).
[29] J. S. Hur, E. S. G. Shaqfeh, and R. G. Larson, J. Rheol. **44**, 713 (2000).
[30] R. B. Bird, C. F. Curtiss, R. C. Armstrong, and O. Hassager, *Dynamics of Polymeric Liquids: Kinetic Theory* (John Wiley and Sons, New York, 1987), Vol. 2.
[31] By "nonaffine" we mean the polymer molecule does not follow the streamlines of the flow and moves with smaller velocity than the imposed flow. To be accurate, truly affine deformation—moving like a fluid element (not only moving along the streamlines but also with the same imposed velocity)—is achieved only at high Wi at small strains and was not observed at the Wi studied.
[32] E. C. Lee, M. J. Solomon, and S. J. Muller, Macromolecules **30**, 7313 (1997).
[33] A. Link and J. Springer, Macromolecules **26**, 464 (1993).
[34] The FFT was calculated after subtracting the mean extension from all of the data points and multiplying the data by a Welch window function [W. H. Press *et al., Numerical Recipes in C* (Cambridge University Press, Cambridge, 1988), p. 442]. The PSD for all of the data sets for a given condition were averaged together and normalized according to Parseval's theorem.
[35] M. Doi and S. F. Edwards, *The Theory of Polymer Dynamics* (Oxford University, Oxford, 1986).